IEEE Access
Multidisciplinary | Rapid Review | Open Access Journal

Received February 7, 2018, accepted March 19, 2018, date of publication April 2, 2018, date of current version April 25, 2018.

Digital Object Identifier 10.1109/ACCESS.2018.2821717

Mapping MODIS LST NDVI Imagery for Drought Monitoring in Punjab Pakistan

JAHANGIR KHAN, PENGXIN WANG, YI XIE, LEI WANG, AND LI LI
[1]Key Laboratory of Remote Sensing for Agri-Hazards, Ministry of Agriculture, Beijing 100083, China
[2]College of Information and Electrical Engineering, China Agricultural University, Beijing 100083, China

Corresponding author: Pengxin Wang (wangpx@cau.edu.cn)

This work was supported by the National Natural Science Foundation of China under Grant 41371390.

ABSTRACT A near-real-time drought monitoring approach termed as vegetation temperature condition index (VTCI) and a geospatial near-real-time coupling (NRTC) approach were applied to investigate drought over the great plain of Punjab, Pakistan. We identified the warm edges (LST_{max}) and cold edges (LST_{min}) as well as determined and validated the drought on a time series (2003–2008) of satellite EOS's MODIS-Aqua data products. We assessed six years of drought conditions during the winter-wheat-growing seasons and determined the effects of the record-breaking drought during 1998–2002 and its impact on the 2003–2008 periods. The VTCI drought monitoring approach is based on the integration of the normalized difference vegetation index and land surface temperature for comprehensive coverage of current drought and edges determination. The geospatial NRTC approach, which utilizes the VTCI imagery and daily precipitation data, was used for the validation of drought over five weather stations. It was established that the VTCI result has a higher correlation coefficient (r) with cumulative precipitation ($r = 0.88$) in the winter, during the six-year period of the Julian day of year (D-041), whereas the D-169 correlation was found to be negative in the summer, as the thermal boundaries gradually increases, which indicate the seasons and time of the days. The drift finding indicates that the VTCI not only achieves results that are very close to the recent precipitation anomaly but also correlates on the past precipitation. This analysis shows the good sensitivity of the VTCI to soil moisture and precipitation in agricultural areas. Our results suggest the capability of the VTCI for near-real-time drought monitoring as a better indicator of vegetation and thermal conditions over the regions in both rainfed and irrigated covenant areas.

INDEX TERMS Drought determination, drought validation, vegetation temperature condition index, warm and cold edges.

I. INTRODUCTION

Drought is an insidious and creeping hazard with a prolonged scarcity and dearth complex nature that results from meager annual precipitation. The drought had always implicated great impacts on the agricultural, meteorological, ecological and socio-economic spheres of the world [1], [2]. The accurate drought appraisal and monitoring approach closely depend on the measurement of rainfall and superficial water contents, both regionally and globally, for drought monitoring [3]. It is important that preparation for drought should be an integral part of environmental policies and the development of dynamic and near-real-time drought monitoring approaches are pivotal [4]. The stochastic characterization of drought requires inquiries into a series of innovations to introduce perfect indices for drought monitoring, and also to frame and model the extreme concurrent changes of the land with multivariate indices [4]–[6].

At first, the traditional palmer drought severity index (PDSI) was used to monitor the drought conditions from available temperature and precipitation data to estimate the relative dryness and wetness for long-term drought quantification [7]. Beside PDSI, the standardized precipitation index (SPI) is a probability index that characterizes the abnormal wetness and dryness for the dry spell monitoring on monthly or longer duration [8]. In contrast, various studies have employed remote-sensing data to acquire land surface conditions. Dai [9] addressed the spatial hydro-meteorological indices for aridity changes in present and past, and he determined

the major problems leading to new variants of the PDSI exhibiting distinct occurrences of soil moisture and drought. Zargar *et al.* [10] presented more than seventy drought indices, which describe the research directions for different types of drought, including meteorological, agricultural, and hydrological droughts. Traditional techniques of drought estimation and observation rely on rainfall data and surface water balance components which are often limited in a region [11], [12]. Exclusive satellite-driven-indices like NDVI have evolved considerably for enduring and monitoring droughts [13]–[15].

The NDVI is amongst the indices that are based on the most fundamental scientific principles [16]. The NDVI is a well-dispersed, assembled index for determining the significance of drought conditions [17]. The NDVI can be a useful index for vegetation and ecosystems in semi-arid environments, where vegetation covers less than 30 percent of the area [17]–[19]. Kogan [13] used NDVI for the expansion of the VCI that showed success when applied to drought detection, and also coupled the vegetation condition index (VCI) and temperature condition index (TCI) for drought monitoring, duration and intensity. However, Kogan concluded that the VCI is not sufficient for accurate drought investigation. Therefore, NDVI is invoked to provide a robust measure of the presence and abundance of vegetation in a wide range of environmental conditions, along with the LST for thermal fluxes. This index is very useful for monitoring rainfall dynamics in semi-arid and arid areas. LST signifies a great extent condition of the surface with the vigorous extraction of heat fluxes, thermal properties and receives attention in climatological and ecosystem research as the fundamental indicator of the land surface physical changes [20], [21]. Monitoring the states of the land cover, crops and vegetation, the LST is used as a key indicator of the energy fluxes into the atmosphere and ground for the calculation of drought conditions [22], [23].

The temporal variability of NDVI and surface radiant temperature (Ts), with its biophysical variables to examine variation in the relationship between NDVI and Ts in regard to spatial and temporal properties of the observations, has been determined [24]. The triangle/trapezoid method using the NDVI and Ts for obtaining energy fluxes and surface soil water content has been used [25]. Similarly, Wan *et al.* [26] and Sun *et al.* [27] utilized the NDVI and LST using the maximum value compositing (MVC) method for drought monitoring and identification of the warm edges (LST_{max}) and cold edges (LST_{min}) using the VTCI approach over the southern Great Plain of the U.S. and Guanzhong Plain of China.

The spatial pattern of the LST and NDVI are utilized by temperature vegetation dryness index (TVDI) to determine the dry-edge and wet-edge in relationship to disclose temporal changes of the land surface soil moisture and drought conditions [28], [29]. The uncertainty of TVDI is larger for high NDVI values, where the TVDI isolines are closely set, and also the estimation of the TVDI parameters are problematic in the dry season [29]. The downscaling and artificial intelligence (AI) approaches are considered due to limitations in TVDI and VTCI with the spatial resolution to estimate the soil moisture contents in the eastern province of Iran [30]. TVDI can be used in heterogeneous landscape for soil moisture and drought assessment [17], whereas, VTCI is favorable for cropland under both rainfed and irrigated conditions to identify the soil moisture and drought conditions [26], [27], [31]. Generally, the TVDI concept is in agreement with temperature-vegetation index (TVX), and in a negative relation to water condition [29]. In contrast, the VTCI concept is in agreement to Kogan [13].

Patel *et al.* [31] used VTCI approach to examine drought conditions using the space plots of the land surface temperature (T_s) and NDVI data products over the Gujarat State of India; they observe a negative correlation for NDVI-T_s and provide drought pattern changes over space and time. VTCI was also found to be related to crop yield anomalies occurring due to drought conditions and it has been observed as an ideal index for agricultural drought monitoring [31]. The VTCI is used in comparison to other remote-sensing drought indices (e.g., NDVI, LST, VCI and TCI) with more accuracy in drought assessment [14]. The VTCI drought imagery for drought forecasting has been used in Guanzhong Plain of China [32]. Furthermore, Adnan *et al.* [35] and Haroon *et al.* [33] found severe drought during 1998-2002 in the region. Haroon *et al.* [33] employed drought severity index (DSI) to investigate drought conditions in Pakistan.

We employed the VTCI approach, which incorporates the LST and NDVI for drought monitoring, as well as for warm and cold edges over the plain of Punjab. We demonstrated the differences of wet and dry drought conditions; VTCI reflected the soil moisture information for single-year and multiyear (i.e., the warm edges and cold edges are determined by using single-year and multiyear composite LST and NDVI products in a certain period). This study determined the drought conditions using VTCI approach based on Moderate-Resolution Imaging Spectroradiometer (MODIS) NDVI and LST data products for agricultural drought monitoring. Besides the determination and validation of drought, we categorized the drought and identified the warm and cold edges of the cropland areas under both rainfed and irrigated conditions for the six-year period during the winter-wheat-crop seasons (2003-2008). The exposed VTCI drought imagery is validated quantitatively with a geospatial near-real-time coupling (NRTC) approach using daily precipitation data over five stations. It is shown that the relationship between the near-real-time VTCI and NRTC is an effective approach for the rapid assessment and validation of droughts. Our analysis clearly shows that the NDVI, LST, and VTCI are very reasonable for drought monitoring during the winter-wheat-crop season in the cropland area of Punjab.

II. STUDY AREA

Pakistan lies in the south Asian region, where the reliance on precipitation data is not sufficient for drought monitoring.

This is due to the lack of reliable and complete data and proper information network systems, and the lower availability of weather-stations in Pakistan. In Pakistan, drought occurs mainly due to the shortfall of rains coming from southwest monsoons, which seem to be associated with climatic La-Nina/El-Nino sibling events [34]. Droughts are frequently experienced in the southern parts of the region. ENSO has a direct impact on drought and flood in the region, with a negative impact of rainfall in the summer on irrigated agricultural lands of Pakistan [34], [35].

The Punjab area experienced the severe droughts during 1899, 1920 and 1935. The northeast and west of Pakistan faced the severe droughts in 1902 and 1951, while the southeast faced the severe droughts in 1871, 1881, 1899, 1931, 1947 and 1999, respectively [35], [36]. In 1952, the drought was the most severe in the continent, and the long-lasting drought period was recorded during 1998-2002 [33], [35]. Due to the variability of annual precipitation, the plain is susceptible to droughts in the spring and early summer, as the plain is a semi-arid and semi-humid region.

The geographic location of Pakistan is approximately 23-37°N and 60-79°E, in the western zone of south Asia. Pakistan is located along the Arabian Sea in the south and is bordered by China to the northeast, India to the east, Iran to the southwest and Afghanistan to the west. The plain of Punjab has an area of approximately 205,344 km^2, with an alluvial plain with an altitude of approximately 100-260 meters above sea level [37]. The region's climate is dry, with an annual precipitation gradient from 100 mm in the south to 600 mm in the northwest, which reaches up to 1000 mm along the north-eastern border and, during the Rabi season, typically ranges from 200 mm to 500 mm and can reach up to 800 mm under heavy rainfall [35]–[37]. Pakistan produces rice and wheat crops, with rotation cropping systems. The major crops of cotton-wheat and rice-wheat systems occupy almost 60 % of the wheat. Due to the climatic changes and global warming in the world, recurring droughts and weather test patterns influence crop yields in Pakistan [36], [37].

The current study focused on 518 × 598 km square area of the agricultural land positioned over the area of (28.42-32.98°N, 70.14-75.39°E) as shown in (Fig. 1) located at https://www.star.nesdis.noaa.gov/smcd/emb/vci/VH/vh_browseByCountry_province.php?country_code=PAK&province_id=7. Further, the locations of the five meteorological stations over the cropland of Punjab were obtained with their names and coordinates. The cropland's south stations resides two weather-stations in Multan defined as MLN 1 and MLN 2 located at (30.12°N, 71.26°E and 30.25°N, 71.44°E) and the two weather-stations at centre of region in Faisalabad called FSD 1 and FSD 2 located at (31.25°N, 73.08°E and 31.26°N, 73.44°E) and the northeast station resides one weather-station located in Lahore called the LHR at 31.35°N, 74.24°E respectively.

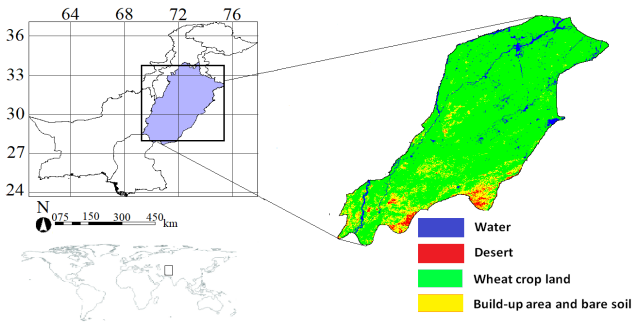

FIGURE 1. The geographic location of the cropland of Punjab, 518 x 598 square km at 1 km pixel size land product spatial resolution mapped over h24/v05 and h24/v06 plates.

III. MATERIAL

NOAA's EOS continuous streams of MODIS data products provide intact information on the atmosphere, land and ocean processes towards a particular goal, to integrate the earth's terrestrial and Polar Regions to monitor the entire land cover [38]. The MODIS data products quantify the characteristics of the land surface, especially the land and snow cover extents as well as the leaf area, and covers fire occurrences in terms of quantifying and validating the ecosystem processes. The MODIS sensor resides aboard on the Terra and Aqua platforms, which were launched in December 1999 and May 2002, respectively, covering the earth's surface in one to two days with 36 spectral bands, with custom-tailored spectral bands of 0.4-14.4 μm and delivering 29 bands at 1000 m, 5 bands at 500 m, and two bands at 250 m spatial resolution located at https://modis-land.gsfc.nasa.gov/ [39].

To develop the data for global research, the orbit equator changes for the MODIS Terra (EOS AM) passes from north to south in morning, and Aqua (EOS PM) passes from south to north in the afternoon, this defines the earth observatory system (EOS) and earth science respectively. In this work, we selected the MODIS-Aqua data products due to time variations and land surface conditions in the region. Due to the temperature extremes in this equator, in afternoon time the surface soil moisture and drought conditions could be characterized more vigorously as compared to the morning time [40]. The MODIS-Aqua emissivity values per pixel area with a sequence of swath-to-grid-based global products are measured as a sinusoidal projection. The MODIS-Aqua data products MYD13A2 (NDVI) and MYD11A2 (LST) are employed for this calculation located at https://lpdaac.usgs.gov/ [40], [41]. The acquired MODIS LST data product over 8-day intervals and NDVI data products with 16-day intervals at 1 km spatial resolution (1 km Integerized Sinusoidal grid in nominal 926.62543305 m) are located at https://earthexplorer.usgs.gov/. The latitude and longitude of the study area are set to 30°N and 75°E with Lambert Azimuthal projection for the horizontal tile 24 along with vertical tile 5 and 6 (i.e. h24v05 and h24v06) located at https://modis.gsfc.nasa.gov/related/organigram.php.

We selected the MODIS-Aqua data products with 16-day composite LST and NDVI, during the period

2003-2008 and were recorded during the winter-wheat-crop season. The LST and NDVI approximate the VTCI values that determine the amount and distribution of vegetation on the land surface temperature. In response, the reflective bands, namely, red (620-670 nm) for band 1 and near-infrared (841-876 nm) for band 2, and the emissivity bands, in accordance with descriptions of (10.780-11.280 μm) for band 31 and (11.770-12.270 μm) for band 32 in particular, are utilized in this study. Besides, the VTCI approach was applied at 16-day and 10-day interval using LST and NDVI data products for drought monitoring in U.S. and China, respectively [26], [27]. In this study, the VTCI drought monitoring approach was applied in the region at 16-day interval using the LST and NDVI data products in a given time series.

In our study, the mapped VTCI imagery values over five weather-stations are carried out for the validation of drought along with daily ground measured precipitation anomaly in the cropland of the plain. The available daily precipitation data over the five stations at 1 km pixel area are measured in millimeter (mm) with certain periods, from 16-day to one-year cumulative precipitation anomaly during the period of 2002-2008. The VTCI values correlate to the past precipitation anomaly in the validation of drought. The VTCI imagery day of years (D) is presented in our studies in accordance with Julian Day (JD) for the determination and validation in given time series [42].

IV. METHODOLOGICAL DESCRIPTION OF THE NDVI, LST AND VTCI METRICS

The VTCI approach exposes the plots residing in LST-NDVI space are the most appropriate method for the determination of drought as well as the identification of warm and cold edges. Hence the warm and cold edges express the soil moisture conditions in trapezoidal (i.e., LST-NDVI) feature space. The triangular or trapezoidal region, which is called the LST-NDVI feature space, covers the vegetation and soil thermal content, as the warm edges and cold edges in a time series of VTCI, shows the variations of vegetation and temperature and to present the changes in time/seasons (Fig. 2). Hence, the variations in the uppermost extent of the plots represent the warm edges, and the bottom represents the cold edges. Where LST_{min} is the minimum land surface temperature (cold edge), and LST_{max} is the maximum land surface temperature (warm edge), presented in (Fig. 2) [26], [27].

The LST-NDVI space plot absolute values of the oblique courses of the warm edges are in accordance with the variations of temperature and area-specific and shows variations in soil properties. The processed information's for the cold edge in parallel to NDVI (i.e., zero gain in cold edges as LST_{min}), whereas, the warm edge in a relation to NDVI. Consequently, the determination of VTCI drought imagery in response to soil moisture is based on the integration of LST and NDVI products using single-year data in a certain period.

Fig. 2 represents the conceptual LST-NDVI feature space, with LST plotted as a function of NDVI. The left edge present the bare soil from the range top-to-down (dry-wet).

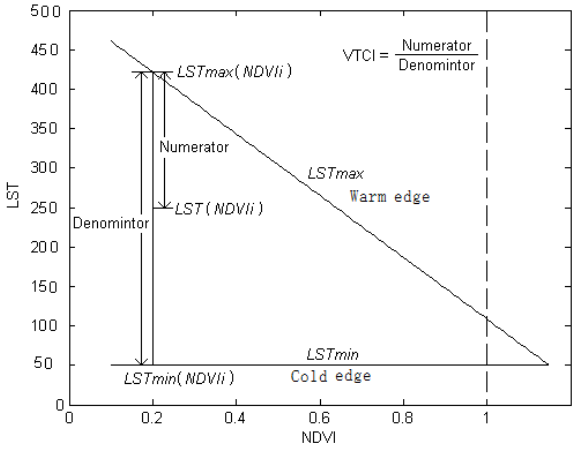

FIGURE 2. Schematic illustration of VTCI modeled LST-NDVI space.

As long the green vegetation amount increases along the NDVI (x-axis), the maximum-surface-temperature reduce, whereas, the upper edge defines the negative relationship in dry conditions, which present the upper limit to surface temperature. The determination of VTCI drought and the warm and cold edges for single-year and multiyear using the composite LST and NDVI products in a study area with the following processes:

1) In Fig. 2 the numerator is the differences between maximum LST of the pixels and LST of one pixel, whereas, in the denominator the difference between the maximum and minimum LSTs of the pixels, by using single-year composite LST and NDVI products for the drought imagery as well as warm and cold edges in a certain period.

2) The edges are determined by using the multiyear maximum-value composite LST and NDVI products in the certain period.

3) The warm edge is determined by incorporating the multiyear maximum-value composite LST and NDVI products. The cold edge is determined by using the multiyear maximum–minimum-value composite LST products and the multiyear maximum-value NDVI products, called the maximum-minimum-value compositing approach for determining the cold edge, based on the structural design of the VTCI approach (Fig. 2) [27].

To determine drought as well as warm edges and cold edges in a triangular space, integrating LST versus NDVI, the MVC method was adopted in our approach to obtaining the composite LST and NDVI data in the specified period [27].

Mapping the MODIS VTCI imagery for drought monitoring as well as to identifying the warm and cold edges, we employed the composite 16-day LST and 16-day NDVI products for this calculation. Plotting of the LST and NDVI products are proposed in a variety of conditions to characterize the quantitative measures of drought and soil moisture conditions in a trapezoidal manner. The LST-NDVI space plots are negative in relation to the crop moisture index, which indicates that the LST and NDVI are sensitive to the

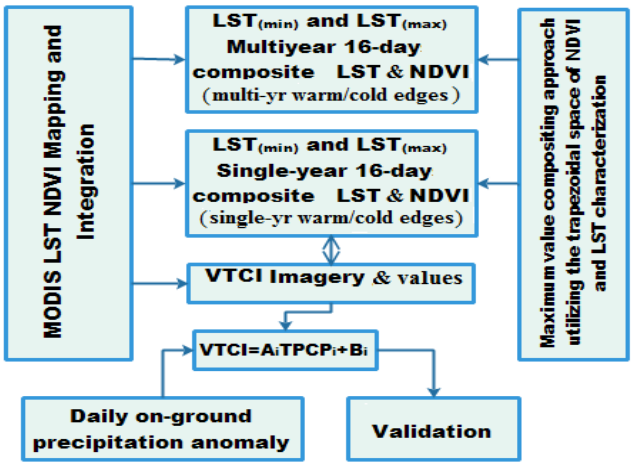

FIGURE 3. Schematic methodological diagram for the VTCI drought, warm and cold edges and linear correlation coefficient (r) values abstraction using MODIS LST and NDVI data products and accumulative precipitation anomaly (TPCP) in certain periods for the determination and validation of drought conditions.

surface moisture conditions [43]. For adequate plotting and location of warm and cold edges, graphical representations are examined, with variations of vegetation and heat fluxes based on the LST and NDVI variables using the VTCI as a drought monitoring approach for the 6-yrs period (Fig. 3). The MVC method to firmly resolve the observance of single-year and multiyear composite LST and NDVI products to determine and validate the drought as well as to identify the warm and cold edges, presented in (Fig. 2) and (Fig. 3), respectively.

The VTCI approach defines the ratio of LST differences among pixels (the numerator is the difference between maximum LST of the pixels and LST of one pixel, the denominator is the difference between maximum-and-minimum LST of the pixels) with a specific NDVI value in a defined area [26], [27], [32].

$$VTCI = \frac{LST_{NDVI_i \cdot \max} - LST_{NDVI_i}}{LST_{NDVI_i \cdot \max} - LST_{NDVI_i \cdot \min}} \quad (1)$$

where

$$LST_{NDVI_i \cdot \max} = a + bNDVI_i \quad (2)$$

$$LST_{NDVI_i \cdot \min} = a' + b'NDVI_i \quad (3)$$

Hence, $LST_{NDVIi.max}$ and $LST_{NDVIi.min}$ are the maximum and minimum LSTs of pixels that have the same $NDVI_i$ value in the study region. In particular, LST_{NDVIi} denotes the LST of a single-pixel whose NDVI value is $NDVI_i$. The coefficients a, b, a' and b' can be estimated from an area that is large enough that the soil moisture at the surface layer spans from the wilting point to the field capacity at the pixel level, as in (1). Generally, the coefficients are estimated from the scatter plots of the LST and NDVI in the area. Equations (2) and (3), define the tentative judgment indicator in the form of scatter plots, whereas the NDVI and LST are utilized in various composite LST and NDVI products. In addition, the coefficients of a, b, a' and b' appraises the estimated VTCI space plots of the LST and NDVI in account of the comprehensive region, and accomplish the dryness and wetness of soil over the superficial horizon extent of wilting position at pixel level geospatially using the MVC method. VTCI can be perceptible and conceivable as the ratio of LST differences through the midst of pixels with peculiarity to NDVI value in an area.

The VTCI drought monitoring approach unifies the remotely-sensed radiant fluxes in accordance with a specific wavelength and thermal values and gives a transformation involving the LST and NDVI. The observed surface temperature of LST is considered in Kelvin (k).

The NDVI can be calculated as

$$NDVI = \frac{\rho_{NIR} - \rho_{red}}{\rho_{NIR} + \rho_{red}} \quad (4)$$

where ρ_{red} and ρ_{NIR} are the reflectance band 1 and band 2, respectively.

Subsequently, the VTCI values were grouped into four drought intensities, each of which has different ranges of values for the categorization of drought: normal or wet (1 to 0.57), slight-mild drought (0.56 to 0.44), moderate drought (0.43 to 0.38), and severe drought (0.37 to 0) [32].

Furthermore, for the validation, a geospatial NRTC approach is proposed to retrieve VTCI imagery values along with the daily precipitation multiyear data anomaly to obtain a more accurate relationship (linear correlation coefficient). The NRTC retrieves the pixel areas of the VTCI values and correlates them with the daily on-the-ground precipitation data within a certain period. The linear correlation coefficient value corresponds to the VTCI and daily cumulative precipitation values within certain periods, during 2003-2008 for VTCI values and 2002-2008 for precipitation anomaly.

$$VTCI = A_i TPCP_i \text{ x } B_i \quad (5)$$

Where

$$TPCP_i = \sum_{i=1}^{n} TPCPi$$

Where VTCI express the difference between $LST_{NDVI_i \cdot \max} - LST_{NDVI_i}$ and $LST_{NDVI_i \cdot \max} - LST_{NDVI_i \cdot \min}$ and the TPCP is the accumulative precipitation in a certain period (TPCPi) from 16-day to 12-month. Here A is the slope or gain and B is the offset in the specified period, i.e., 16-day VTCI imagery (D-009 to D-169) values during 2003-2008, in consideration with TPCP anomaly from (16-day to12-month) during 2002-2008.

For the validation of drought, we set the TPCP anomaly periods of (16-day, 1-, 2-, 3-, 4-, 5-, 6-, 9- and 12-month) to (16-, 32-, 64-, 96-, 128-, 160-,192-, 288- and 384-day) respectively (i.e., TPCPi anomalies are multiple of 16-day in the given period due to 16-day VTCI imagery intervals from D-009 to D-169 during 2003-2008). Generally, the satellite VTCI imagery (D-009, -025, -041, -057, -073, -089, -105,

-121, -137, -153, -169) during 2003-2008 are coupled geospatially (in relation) with accumulative precipitation anomaly (TPCP) in the periods of 16-, 32-, 64-, 96-, 128-, 160-, 192-, 288-, and 384-day during 2002-2008 respectively, based on the linear regression, as in (5). Hence, in linear correlation analysis, the VTCI imagery values correlate to the recent and past precipitation.

Furthermore, the NRTC approach retrieves the pixel-area values of the VTCI imagery at 1 km spatial resolution and establishes a correlation with the TPCP data (the input data should be in matrix format) over five weather-stations, to obtain the values of (r) between the VTCI and TPCP on a near-real-time basis in the given time periods. This utilized VTCI and TPCP anomaly using the NRTC geospatial approach for the validation of drought.

TABLE 1. Equations for the determination of drought and edges for single-year and multiyear from D-009 to D-169 during 2003-2008.

Day of years	Warm edges	Cold edges
009	$LST_{NDVi\,min} = 287 + 0\ NDVI_i$	$LST_{NDVi\,max} = 318 - 24\ NDVI_i$
025	$LST_{NDVi\,min} = 288 + 0\ NDVI_i$	$LST_{NDVi\,max} = 320 - 19\ NDVI_i$
041	$LST_{NDVi\,min} = 289 + 0\ NDVI_i$	$LST_{NDVi\,max} = 325 - 24\ NDVI_i$
057	$LST_{NDVi\,min} = 292 + 0\ NDVI_i$	$LST_{NDVi\,max} = 334 - 30\ NDVI_i$
073	$LST_{NDVi\,min} = 294 + 0\ NDVI_i$	$LST_{NDVi\,max} = 335 - 25\ NDVI_i$
089	$LST_{NDVi\,min} = 298 + 0\ NDVI_i$	$LST_{NDVi\,max} = 341 - 30\ NDVI_i$
105	$LST_{NDVi\,min} = 300 + 0\ NDVI_i$	$LST_{NDVi\,max} = 341 - 30\ NDVI_i$
121	$LST_{NDVi\,min} = 300 + 0\ NDVI_i$	$LST_{NDVi\,max} = 341 - 30\ NDVI_i$
137	$LST_{NDVi\,min} = 300 + 0\ NDVI_i$	$LST_{NDVi\,max} = 341 - 30\ NDVI_i$
153	$LST_{NDVi\,min} = 300 + 0\ NDVI_i$	$LST_{NDVi\,max} = 350 - 39\ NDVI_i$
169	$LST_{NDVi\,min} = 300 + 0\ NDVI_i$	$LST_{NDVi\,max} = 350 - 31\ NDVI_i$

Warm edges (thermal boundary as LST_{max} gain and offset), while zero gain in cold edges as LST_{min}.

V. RESULTS AND DISCUSSION

A. DETERMINATION OF DROUGHT AND 'WARM AND COLD EDGES'

VTCI drought monitoring approach implies the sensations of the heat fluxes physical exertion and establishment of detachment for the warm and cold edges and drought determination over the area. The acquired data, which cover the wheat-crops land of Punjab, Pakistan, is utilized for the vegetation and thermal fluxes of the MODIS LST and NDVI data product, to identify the edges and droughts conditions through the following processes:

1) The composite LST and NDVI data products are combined by using single-year products for the warm and cold edges in a certain period. The creation of the composite LST and NDVI data products using multiyear maximum-value results in the determination of warm edge. By using multiyear maximum-minimum-value composite LST products and a multiyear maximum NDVI product results in the detection of cold edge, this is called the maximum-minimum-value compositing approach for the determination of cold edges during the period from D-009 to D-169 spanning 2003-2008, and here the selected plots at D-041 in the given period with no water stress are presented in [Fig. 4 (a)] and [Fig. 4 (b)]. The absolute values of the oblique courses of the warm and cold edges are in accordance with the variations in wet and dry conditions, due to the prevalence of the vegetation and land cover type in the given periods of time/seasons.

2) Time-series characteristics of the VTCI are considered to establish the warm and cold edges more accurately for single-year in response to soil moisture and drought. Whereas, the warm and cold edges using multiyear's in response to soil moisture with no VTCI drought imagery. In D-041 during 2003-2008 using multiyear composite LST and NDVI for the warm and cold edges expose the soil moisture conditions are presented in [Fig. 4 (a)] and [Fig. 4 (b)]. In contrast, the single-year composite LST and NDVI products are used to identify the warm and cold edges at D-041 in the year 2005 and 2007 in response to soil moisture conditions are presented in [Fig. 4 (c)] and [Fig. 4 (d)]. An unbalanced temperature increase is observed from the winter season into the summer season in the entire period, using single-year and multiyear data products from D-009 to D-169 during 2003-2008. The drought and edges results depend on the variations in wet and dry conditions of the plain. Equations (1), (2), and (3) define the (soil moisture and drought conditions) based on the equations of (Table 1). Generally, the coefficients of Equations (2) and (3) were estimated from scatter plots of LST and NDVI using different composite LST and NDVI products in the given periods for single-year and multiyear using (Table 1) for these calculations from D-009 to D-169 during 2003-2008.

3) VTCI drought imagery of each 16-day composite LST and NDVI data have been used for drought monitoring, using single-year maximum-minimum 16-day LST composite data products along with single-year maximum 16-day NDVI data products, which reveal the drought imagery at D-041 in each year during 2003-2008 presented in [Fig. 5 (a)] to [Fig. 5 (f)]. To categorize the drought over five stations the VTCI values from D-009 to D-169 during 2003-2008 are shown in (Fig. 6) calculated from the equations presented in (Table 1).

The equations for the multiyear warm and cold edges are set to single-year warm and cold edges in response to soil moisture and VTCI drought imagery from D-009 to D-169 during 2003-2008 (Table 1). Equations of (Table 1) reveal the temporal changes of the land surface soil moisture and drought conditions in the plain.

For warm and cold edges as well as drought conditions, 154 images were considered for these calculations. For the multiyear's warm and cold edges of the 22 imagery, the two are presented at D-041 during (2003-2008) [Fig. 4 (a) and Fig. 4 (b)]. Whereas the single-year warm and cold edges of the 66 imagery, two are presented at D-041 in the year of 2005 and 2007 [Fig. 4 (c) and Fig. 4 (d)]. Of 66 drought imagery, 6 are presented in (Fig 5) at D-041 during 2003-2008. Further, the VTCIs 66 imagery values over five stations are presented in (Fig. 6) from D-009 to D-169 during

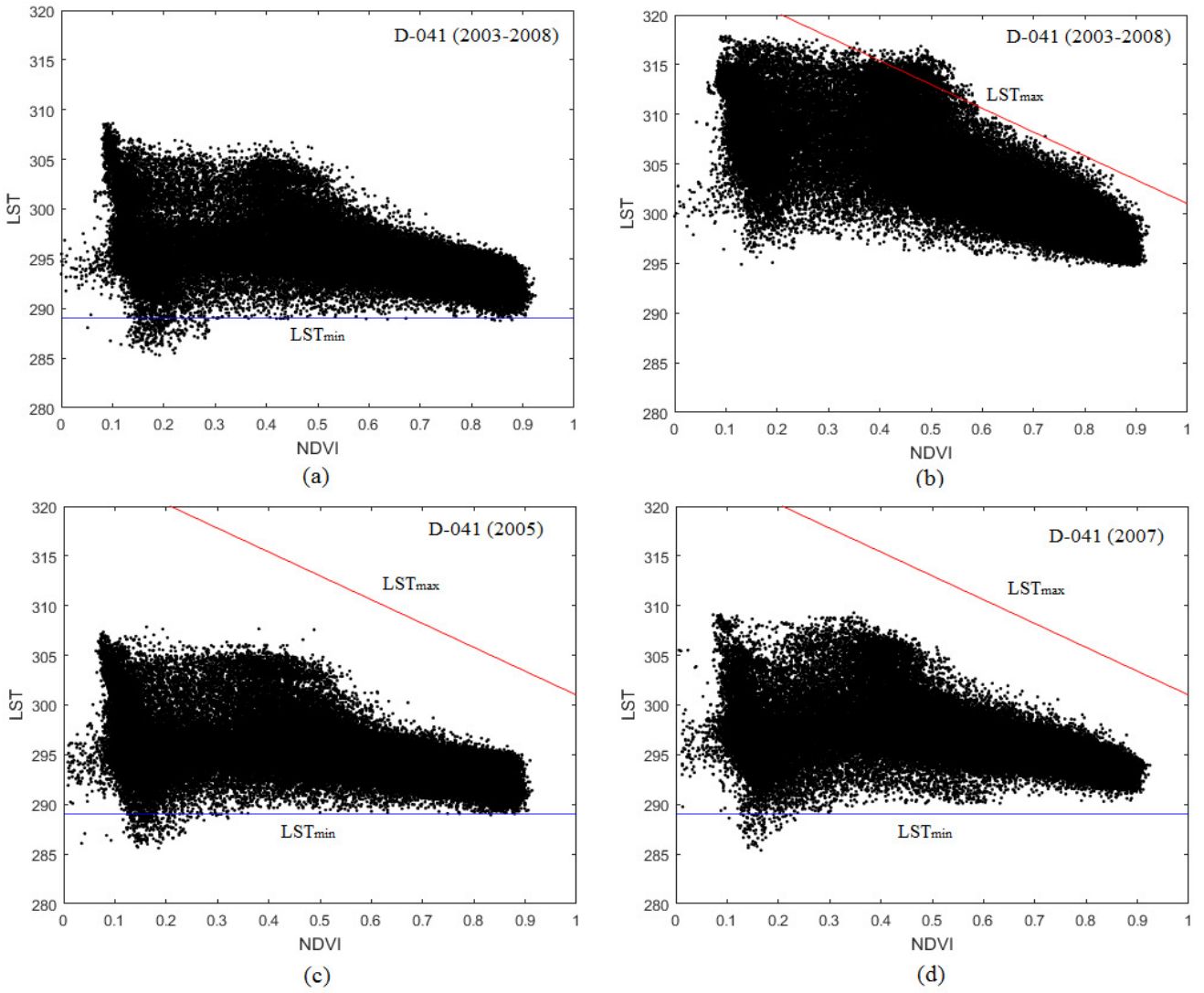

FIGURE 4. Scatter Plots of LST-NDVI at D-041(February first 16-day) in multiyear and single-year during 2003-2008. The determination of the cold edge using the multiyear-maximum-value NDVI products and maximum–minimum-value composite LST products (a) and the determination of the warm edge using the multiyear-maximum-value composite LST and NDVI products (b) and the determination of warm and cold edges using single-year composite LST and NDVI products at D-041 in 2005 (c), and in 2007 (d) respectively.

2003-2008. The presented imagery/values are based on the Equation (1) and (Table 1) in the given periods. Table 1 utilize the Equations (2) and (3) for single-year and multiyear's warm and cold edges. The uppermost plots of multiyear warm edges exist in upper feature space in comparison to multiyear cold edges plots as well as for single-year warm and edges feature plots. The measured coefficients of multiyear warm and cold edges are extent for the single-year warm and cold edges as well as for drought imagery determination and with its validation.

The cropland exhibits distinct occurrences of soil moisture and drought conditions with approximate changes in vegetation and land surface moisture conditions to provide complete information for agricultural practices. In (Fig. 4) the warm edge (LST_{max}) shows less soil moisture availability and shows the dry conditions; in response, the cold edge (LST_{min}) presents no water restriction for plant growth at D-041 during 2003-2008, present the normality.

Therefore, an appropriate method was selected to determine the warm and cold edges, which results in drought, while the VTCI drought is categorized on a scale of (0-1), as shown in (Fig. 5) at D-041 during 2003-2008. At D-041, (Fig. 5) and (Fig. 6) shows the normality or wetness in most of the plain, whereas in the year 2004, a slight-mild drought is observed at FSD 1, MLN 1 and FSD 2 stations, and in the years 2006, the LHR station experienced slight-mild drought, while, in the years 2008 a slight-mild drought was noticed at LHR station. The intensity is described numerically and graphically, accompanied by the drought severity classification and range for each indicator of wetness and dryness, with

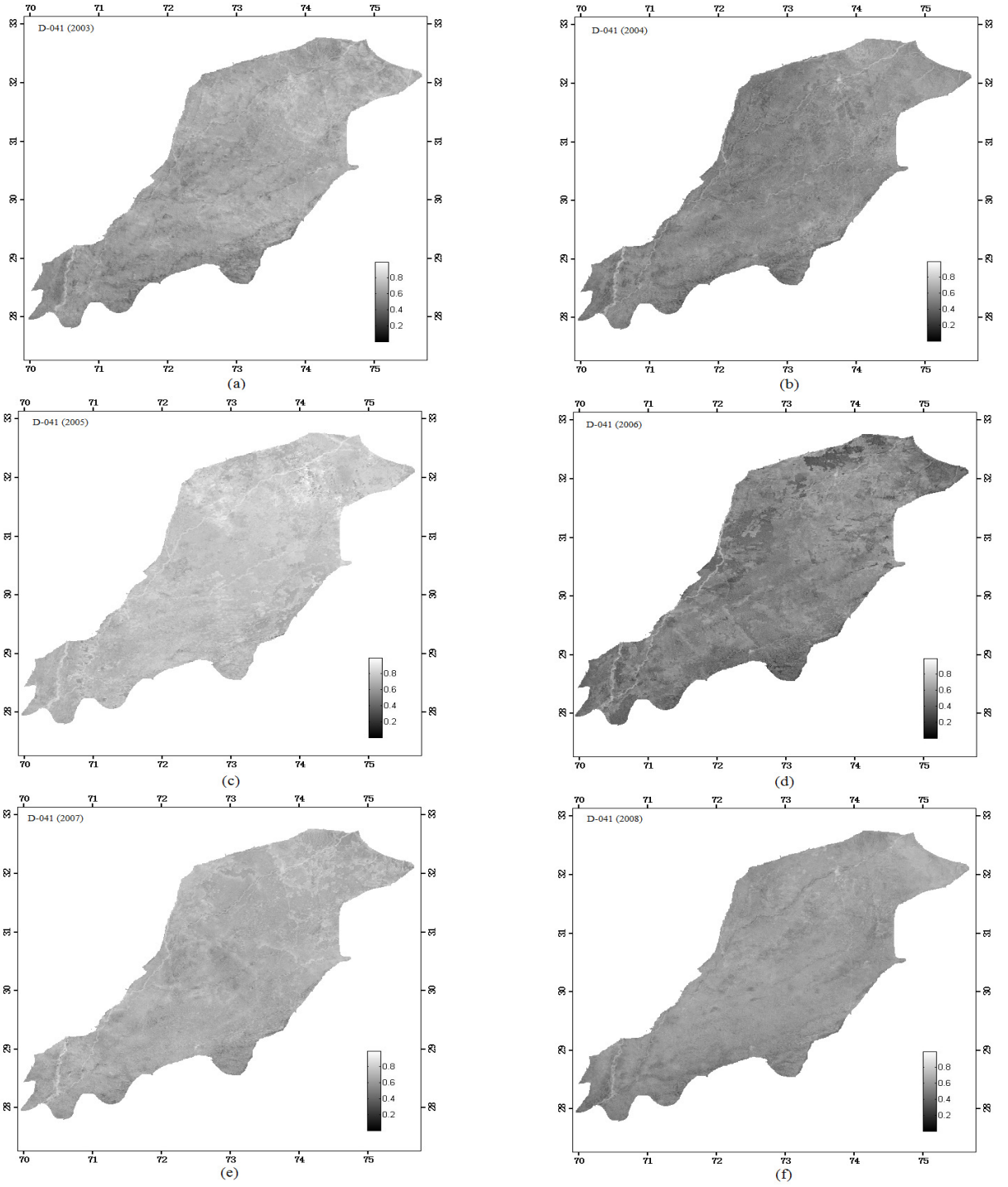

FIGURE 5. **Drought distribution of the cropland in determination of VTCI drought monitoring results in the first 16-day of February (D-041), using the single-year composite LST and NDVI products in the year 2003, 2004, 2005, 2006, 2007 and 2008 are presented in (a), (b), (c), (d), (e) and (f) respectively. The selected images are highly correlated during the winter wheat-crop-growing season at D-041 during 2003-2008; the drought imagery was considered for the cropland of the Punjab Plain.**

consistent big-picture drought conditions to identify the plain in both dry and wet days and years obtainable in (Fig. 5) and (Fig. 6). Fig. 6 covers the VTCI values over the five stations from D-009 to D-169 during a six-year period (2003-2008). Fig. 5 illustrates the understanding of the VTCI drought for the six-year period at D-041 during the crop-growing season, which is essential for comparing and analyzing the VTCI imagery. In general, the classification of the VTCI drought severity depends on the drought characterization: lower the VTCI values, results in severity and high the VTCI values

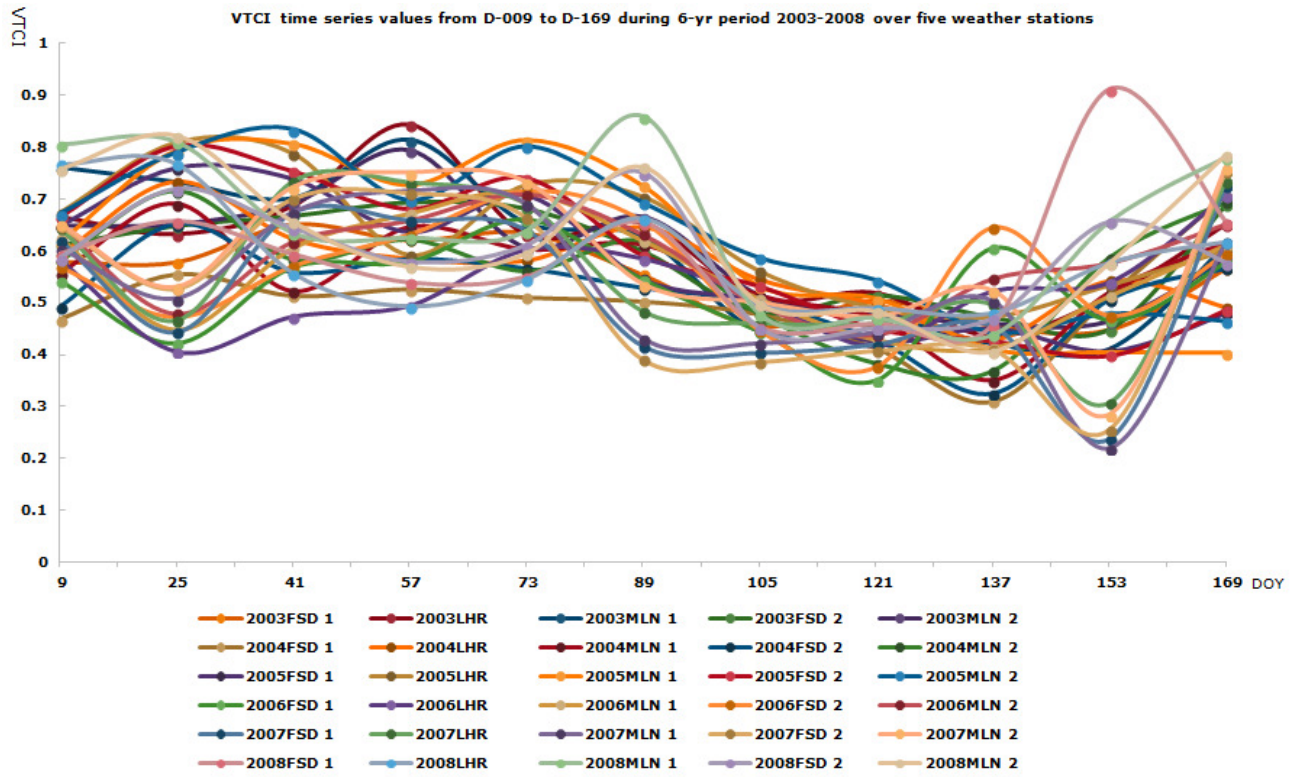

FIGURE 6. VTCI drought disparity and categorization from D-009 to D-169 during six-year periods (2003-2008) over five weather-stations in a scale of 0 to 1 or dry to wet: normality or wetness (1 to 0.57); slight-mild drought (0.56 to 0.44); moderate drought (0.43 to 0.38); severe drought (0.37 to 0).

correspond to the normality. Generally, the VTCI's high value corresponds to (wet area) and low value corresponds to (dry area) (Fig. 6).

The representation of the drought conditions from D-009 to D-169 during 2003-2008 over every five stations are categorized with total VTCI values occurrences (i.e., n = 330) observed in the plain from severe drought to wet or from (0.23 to 1.0). The creative 66 VTCI drought imagery in the given periods were applied in the drought categorizations. Based on the drought classification in the given occurrences, it was established that the severe drought with (n = 12), moderate drought (n = 29), slight-mild drought (n = 111), and normality/wetness (n = 178) VTCI values occurrences' showing of 330 VTCI's occurred values. Fig. 6 presents the VTCI value occurrences from D-009 to D-169 during 2003-2008 and establishes correlations with TPCP anomaly in given periods. These demonstrate the good conditions of normality in the foremost area of the plain as well as reveals that farming conditions are favorable from south to the northeast of the region. This also illustrates that the region had a good irrigation system as well as enough rainfall in the given periods, and play an important role in farming practices in the region.

The result shows that droughts of higher severity are not found over most of the north-eastern, central or southern areas in the Plain of Punjab. According to Adnan *et al.* [35], the northeast and west of Punjab's Plain have variations in precipitation, compared to the southern part of the plain. In the south of the plain, most of the farms with lack sufficient rainfall as compared to the north and northeast, which results in the low and high VTCI values from south to northeast of the plain. This shows that the plain is dependent on the precipitation anomaly even though the plain had the best irrigation system. Base on the 6-yr period results, most of the values are significant, which indicates that the majority of the area shows normal conditions and there is a widespread agreement of rainfed and irrigated conditions over the entire region, which favors optimum farming conditions.

B. VALIDATION OF VTCI DROUGHT

The geospatial near-real-time coupling approach detects the VTCI imagery drought values to validate the drought on a near-real-time basis using precipitation anomaly at each station over the plain of Punjab. The NRTC approach extracts the VTCI values per pixel area to present the VTCI numerical values as well as TPCP values and in response to establish a relationship and offer the (r) values. In general, the NRTC approach extracts the pixel-area of VTCI imagery values in response to accumulative precipitation anomaly to establish a relationship with five stations from D-009 to D-169 during 2003-2008 to validate the drought.

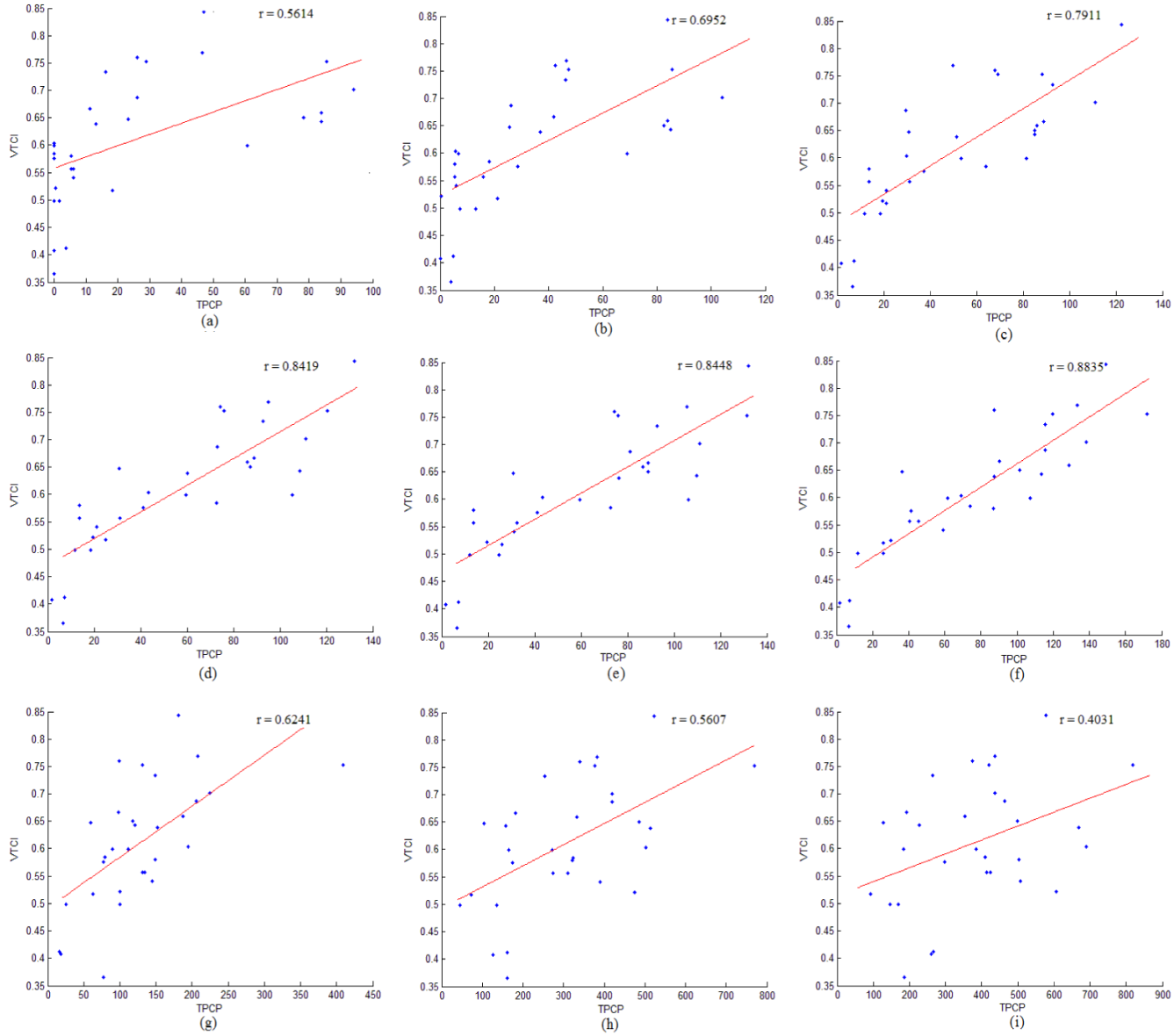

FIGURE 7. Linear Correlation coefficients (r) and plots of the VTCI values at D-041 during 2003-2008 and TPCP anomaly in the periods of 16-day and 1-, 2-, 3-, 4-, 5-, 6-, 9- and 12-month during 2002-2008 at five weather-stations in the plain of Punjab.

At First, by examining the five stations, which are located in the southern, central and north-eastern geographic positions, we assessed the drought and found that there were dry and wet conditions at D-041during 2003-2008 (Fig. 7). Furthermore, considering the determined VTCI drought values and cumulative precipitation anomaly, we found that the VTCI had a very significant relationship with the TPCP from D-009 to D-169 during 2003-2008 in the given periods as shown in (Table 2). The statistical analysis of the cumulative precipitation and VTCI values indicated a significant correlation in the green-up stage during the winter-wheat-crop growing season. The linear correlation at D-041 ($r = 0.88$, $P<0.005$) was the highest with 5-month TPCP (i.e., the relationship of the VTCI drought at D-041 (February first 16-day) during 2003-2008 with 5-month period of accumulative precipitation during 2002-2008, spanning over the given period (Table 2) and (Fig. 7). There was also a significant correlation at the D-041 between the VTCI drought during 2003-2008 and the TPCP during the periods of 16-day, 1-, 2-, 3-, 4-, 6-, 9- and 12-month, during 2002-2008. These periods describe the green-up stages in the D-041 and a significant relationship with 5-month of precipitation anomaly (Fig. 7).

This demonstrates that the VTCI imagery and cumulative precipitation anomaly had a significant correlation. The NRTC approach signifies the relations of VTCI and TPCP values that correlate to past precipitation. Throughout the periods of 16-day to 12-month (TPCPi) values had a significant correlation with the VTCI at the D-041, varying from

TABLE 2. Relationship between VTCI from D-009 to D-169 during 2003-2008 and TPCP in 16-day to 12-month during 2002-2008.

TPCP/VTCI†	16-day	1-	2-	3-	4-	5-	6-	9-	12-month
009	0.3653	0.0687	0.2338	0.2562	0.376	0.2605	0.4151	0.5186	0.4325
025	0.6093	0.7563	0.6532	0.5327	0.4208	0.1578	0.1676	0.288	0.2587
041	0.5614	0.6952	0.7911	0.8419	0.8448	0.8835	0.6241	0.5607	0.4031
057	0.5738	0.6643	0.6527	0.6122	0.5893	0.6021	0.752	0.6893	0.7038
073	0.5402	0.7603	0.7336	0.7335	0.6744	0.6611	0.7345	0.5744	0.596
089	0.5072	0.3509	0.0656	0.2773	0.2657	0.1527	0.1184	0.235	0.3252
105	0.3614	0.2442	0.1568	0.1218	0.1682	0.088	0.0917	0.4467	0.4796
121	0.3556	0.4416	0.3974	0.52	0.6445	0.6257	0.5783	0.5529	0.6227
137	0.2615	0.2052	0.2243	0.5115	0.2925	0.2759	0.2884	0.2500	0.3197
153	-0.0271	0.3104	0.3814	0.4409	-0.2052	-0.0082	-0.1423	-0.1625	-0.0322
169	-0.1243	-0.1227	-0.1532	-0.0725	-0.2662	-0.1778	-0.1998	-0.2364	-0.1706

†The total precipitation anomaly (TPCP) in relation to VTCI imagery values from D-009 to D-196 during 2003-2008. The TPCP anomaly periods of (16-day, 1-, 2-, 3-, 4-, 5-, 6-, 9- and 12-month) were set to 16-, 32-, 64-, 96-, 128-, 160-, 288-, 288- and 384-day during 2002-2008.

0.40-0.88 during 2003-2008 over five stations, as shown in (Table 2) and (Fig. 7). This reveals that the VTCI not only correlates to the recent precipitation but also in a relationship to the elapsed/past precipitation.

Furthermore, the plain of Punjab is rainfed as well as irrigated and, somehow, most of the farms in the northeast are highly rainfed. In the south, most of the farms had lack of rainfall compared to the north. In winter, the linear correlation coefficient between the VTCI and cumulative precipitation for the 6-yr period at D-041 was 0.88, which was highly significant, while at D-169; the correlations were negative as the thermal boundaries gradually increase during the warm or summer season. In late-May and early-June, a negative correlation occurs due to summer seasons. Generally, the relationship between the VTCI and TPCP varies with season. It is positive in the colder season (winter) and negative in the warmer half of the year (summer). The relationship between the VTCI and TPCP becomes negative during late spring for D-153 (May last 16-day) for the 16-day period of precipitation and then over through from four months to one year's accumulative precipitation. The same negative correlation observed at the D-169 (June first 16-day) presented in Table 2. This shows that the relationship between the VTCI and TPCP is usually positive in the winter, as well as in the first sixteen-day of April or early spring, while the relationships are mostly negative in the late days of spring and early days of summer. In particular, the VTCI imagery provides a better map of all locations from D-009 to D-169 for drought monitoring over the plain during 2003-2008.

The VTCI values presented the slight-mild drought and normality in most of the area in winter and early summer seasons over five stations during 2003-2008. Hence, the VTCI time series values under rainfed and irrigated conditions showed better results in the south to northeast regions of the plain, as the measured precipitation data from the southern, central and northern parts of the region were in good relation to drought conditions. In general, the south and center of the plain had less rainfall, and results in low VTCI values, whereas, in the northeast with sufficient rainfall results in high VTCI values, due to which a significant relationship established. This shows that the VTCI values are in good relation with precipitation anomaly and demonstrate that the region is also dependent on the precipitation anomaly. Alongside the plain face water scarcity in the south of the plain and susceptible to drought conditions, whereas, northeast present the normal drought conditions. These results are in good agreement with the above VTCI statistical values and cumulative precipitation anomaly in the given time period.

Even though the plain had so-called a well established irrigated system, but the current study demonstrated that the VTCI values were lower in the south of the plain due less rainfall, whereas, higher in the north of the plain due to enough rainfall anomaly. This shows that the region needs more routing canals and water reservoirs, and should not be reliant on the rainfall anomaly. Due to a shortfall of precipitation, the region might face another severe drought episode (e.g., long-lasting severe drought during1998-2002 in the region/plain) [33], [35]. Besides, Haroon *et al.* [33] used DSI and employed MODIS-Terra monthly data products with monthly precipitation anomaly and presented a good positive relationship in the central part of the country (Punjab plain) from January to May, whereas, in summer season it was not in good agreement in the agricultural areas as well as in the contiguous regions of Punjab. In contrast, the current study is based on the 16-day data products, which signifies our results very accurately with the daily precipitation anomaly (e.g., the MODIS obtained data at D-009 are acquired from (D 009-024) and the obtained precipitation anomaly from (D 009-024) provides more accuracy than in relation with monthly precipitation anomaly from (D 001-030) and so forth). This shows that the VTCI values with daily TPCP anomaly are better than monthly precipitation anomaly for the validation of drought. Therefore, the coupling of VTCI imagery values and the cumulative daily precipita-

tion data show that VTCI and NRTC approach are very promising for detecting daily precipitation anomalies in the plain.

In addition, this work is in widespread agreement with Wan *et al*. [26], in which the LST and NDVI data products were used to generate and validate the vegetation temperature condition index (VTCI) for the monitoring of droughts over the USA's southern Great Plain, and Sun *et al*. [27], in which VTCI was applied on a time-series basis for drought monitoring in China's Guanzhong plain.

The analysis shows that the obtained vegetation and temperature related drought (VTCI) index results are in good agreement with agricultural drought monitoring over the cropland of Punjab, Pakistan.

VI. CONCLUSION

The current study suggests that VTCI is a time-conditioned and area-characterized vegetation index, which is used to obtain the desired results in the cropland area of Punjab. Furthermore, the mapped MODIS NDVI and LST products are very promising in response to soil moisture and VTCI imagery in the plain for drought monitoring as well as to identify the warm and cold edges during the winter wheat-crop-growing season spanning 2003-2008. This shows that VTCI detects the soil moisture status in the region in response to the integration of LST and NDVI, an important indicator of land surface in the region to extract the drought conditions. Results from the current study show that the plain is mostly subjected to wet and slight-mild drought conditions and the recoil states of the warm and cold edges are stable and represent a substantial normality in the region in each year. VTCI illustrate that northeast areas had more surface wetness compare to the south of the plain. In the substantiation of drought, a strong relationship between the VTCI and cumulative precipitation anomaly was found in the cold months, from D-025 to D-057. Whereas, during the warm season at D-169 a negative correlation was established and present the warm/summer season; this indicates that the vegetation and temperature related drought indices might be better for agricultural drought monitoring.

Based on our understandings, the winter-wheat-growing seasons' six-year drought conditions reveal that the affects of the drought conditions with long-lasting record-breaking drought during 1998-2002 impacted the 2003-2008 periods. The effects were categorized mostly normal and present a better drought outlook conditions for farming practices in the region. The VTCI results also exhibited the robustness and accuracy of our method in the region, and show that it might be a better indicator of drought and warm and cold edges than the indices developed from the precipitation anomaly. Also, based on the past and present studies it is concluded that the VTCI approach reveals better results in the croplands plain/areas.

Our work suggests the collection of 16-day data products, that reveal high-quality results rather than one-month data products. The possible suggestions for future studies in this region would be the application of VTCI drought monitoring approach to investigate the drought impact assessment, wheat yield estimation, yield forecasting and drought forecasting in the plain as well as in the contiguous regions of Punjab, Pakistan.

ACKNOWLEDGEMENTS

The authors would like to thank Professor Dr. Zoran Bojkovic, LSM IEEE, for his valuable suggestions. They would also thankful to Pakistan Meteorological Department for providing the precipitation data. This paper was presented at the 37th Canadian Symposium on Remote Sensing, 7–9 June 2016, University of Winnipeg, Canada.

REFERENCES

[1] F. N. Kogan, "Operational space technology for global vegetation assessment," *Bull. Amer. Meteorol. Soc.*, vol. 82, pp. 1949–1964, Sep. 2001.

[2] D. A. Wilhite and M. H. Glantz, "Understanding: The drought phenomenon: The role of definitions," *Water Int.*, vol. 10, no. 3, pp. 111–120, 1985.

[3] W. T. Liu and F. N. Kogan, "Monitoring regional drought using the vegetation condition index," *Int. J. Remote Sens.*, vol. 17, pp. 2761–2782, 1996.

[4] A. AghaKouchak *et al.*, "Remote sensing of drought: Progress, challenges and opportunities," *Rev. Geophys.*, vol. 53, no. 2, pp. 452–480, 2015.

[5] A. Dai, "Increasing drought under global warming in observations and models," *Nature Climate Change*, vol. 3, pp. 52–58, Jan. 2013.

[6] Z. Hao, A. AghaKouchak, and T. J. Phillips, "Changes in concurrent monthly precipitation and temperature extremes," *Environ. Res. Lett.*, vol. 8, no. 3, p. 034014, 2013.

[7] W. C. Palmer, "Meteorological drought," U.S. Dept. Commerce, Weather Bureau, Washington, DC, Res. Paper 45, 1965.

[8] W. C. Palmer, "Keeping track of crop moisture conditions, nationwide: The new crop moisture index," *Weatherwise*, vol. 21, no. 4, pp. 156–161, 1968.

[9] A. Dai, "Characteristics and trends in various forms of the palmer drought severity index during 1900–2008," *J. Geophys. Res., Atmos.*, vol. 116, no. D12, p. D12115, 2011.

[10] A. Zargar, R. Sadiq, B. Naser, and F. I. Khan, "A review of drought indices," *Environ. Rev.*, vol. 19, pp. 333–349, Jul. 2011.

[11] I. U. Din and S. Adnan, "Drought bulletin of Pakistan," Dept. Pakistan Meteorol., Nat. Drought Monitoring Centre, Islamabad, Pakistan, Tech. Rep. 317, Jul./Sep. 2017.

[12] P. S. Thenkabail and M. Gamage, *The Use of Remote Sensing Data for Drought Assessment and Monitoring in Southwest Asia*, vol. 85. Colombo, Sri Lanka: International Water Management Institute, 2004.

[13] F. N. Kogan, "Application of vegetation index and brightness temperature for drought detection," *Adv. Space Res.*, vol. 15, no. 11, pp. 91–100, 1995.

[14] L. Parviz, "Determination of effective indices in the drought monitoring through analysis of satellite images," *Agricult. Forestry/Poljoprivreda i Sumarstvo*, vol. 62, no. 1, pp. 305–324, 2016.

[15] A. J. Peters, E. A. Walter-Shea, L. Ji, A. Vina, M. Hayes, and M. D. Svoboda, "Drought monitoring with NDVI-based standardized vegetation index," *Photogrammetric Eng. Remote Sens.*, vol. 68, no. 1, pp. 71–75, 2002.

[16] C. J. Tucker and B. J. Choudhury, "Satellite remote sensing of drought conditions," *Remote Sens. Environ.*, vol. 23, no. 2, pp. 243–251, 1987.

[17] K. A. Berger, Y. Wang, and T. N. Mather, "MODIS-derived land surface moisture conditions for monitoring blacklegged tick habitat in southern New England," *Int. J. remote Sens.*, vol. 34, no. 1, pp. 73–85, 2013.

[18] H. Schmidt and A. Karnieli, "Remote sensing of the seasonal variability of vegetation in a semi-arid environment," *J. Arid Environ.*, vol. 45, no. 1, pp. 43–59, 2000.

[19] C. J. Tucker, "Comparing SMMR and AVHRR data for drought monitoring," *Int. J. Remote Sens.*, vol. 10, no. 10, pp. 1663–1672, 1989.

[20] S. Park, J. J. Feddema, and S. L. Egbert, "MODIS land surface temperature composite data and their relationships with climatic water budget factors in the central Great Plains," *Int. J. Remote Sens.*, vol. 26, no. 6, pp. 1127–1144, 2005.
[21] Z.-L. Li *et al.*, "Satellite-derived land surface temperature: Current status and perspectives," *Remote Sens. Environ.*, vol. 131, pp. 14–37, Apr. 2013.
[22] Z.-L. Li and F. Becker, "Feasibility of land surface temperature and emissivity determination from AVHRR data," *Remote Sens. Environ.*, vol. 43, no. 1, pp. 67–85, 1993.
[23] J. C. Price, "On the use of satellite data to infer surface fluxes at meteorological scales," *J. Appl. Meteorol.*, vol. 21, pp. 1111–1122, Aug. 1982.
[24] S. Goetz, "Multi-sensor analysis of NDVI, surface temperature and biophysical variables at a mixed grassland site," *Int. J. Remote Sens.*, vol. 18, no. 1, pp. 71–94, 1997.
[25] R. R. Gillies, W. P. Kustas, and K. S. Humes, "A verification of the 'triangle' method for obtaining surface soil water content and energy fluxes from remote measurements of the Normalized Difference Vegetation Index (NDVI) and surface e," *Int. J. Remote Sens.*, vol. 18, no. 15, pp. 3145–3166, 1997.
[26] Z. Wan, P. Wang, and X. Li, "Using MODIS land surface temperature and normalized difference vegetation index products for monitoring drought in the southern Great Plains, USA," *Int. J. Remote Sens.*, vol. 25, no. 1, pp. 61–72, 2004.
[27] W. Sun *et al.*, "Using the vegetation temperature condition index for time series drought occurrence monitoring in the Guanzhong Plain, PR China," *Int. J. Remote Sens.*, vol. 29, nos. 17–18, pp. 5133–5144, 2008.
[28] I. Sandholt, K. Rasmussen, and J. Andersen, "A simple interpretation of the surface temperature/vegetation index space for assessment of surface moisture status," *Remote Sens. Environ.*, vol. 79, nos. 2–3, pp. 213–224, 2002.
[29] Y. Han, Y. Wang, and Y. Zhao, "Estimating soil moisture conditions of the greater Changbai Mountains by land surface temperature and NDVI," *IEEE Trans. Geosci. Remote Sens.*, vol. 48, no. 6, pp. 2509–2515, Jun. 2010.
[30] V. Moosavi, A. Talebi, M. H. Mokhtari, and M. R. Hadian, "Estimation of spatially enhanced soil moisture combining remote sensing and artificial intelligence approaches," *Int. J. Remote Sens.*, vol. 37, no. 23, pp. 5605–5631, 2016.
[31] N. R. Patel, B. R. Parida, V. Venus, S. K. Saha, and V. K. Dadhwal, "Analysis of agricultural drought using vegetation temperature condition index (VTCI) from Terra/MODIS satellite data," *Environ. Monitor. Assessment*, vol. 184, no. 12, pp. 7153–7163, 2012.
[32] M. Tian, P. Wang, and J. Khan, "Drought forecasting with vegetation temperature condition index using ARIMA models in the guanzhong plain," *Remote Sens.*, vol. 8, no. 9, p. 690, 2016.
[33] M. A. Haroon, J. Zhang, and F. Yao, "Drought monitoring and performance evaluation of MODIS-based drought severity index (DSI) over Pakistan," *Natural Hazards*, vol. 84, no. 2, pp. 1349–1366, 2016.
[34] F. Kogan and W. Guo, "Strong 2015–2016 El Niño and implication to global ecosystems from space data," *Int. J. Remote Sens.*, vol. 38, no. 1, pp. 161–178, 2017.
[35] S. Adnan, K. Ullah, and G. Shouting, "Investigations into precipitation and drought climatologies in South Central Asia with special focus on Pakistan over the period 1951–2010," *J. Climate*, vol. 29, pp. 6019–6035, Aug. 2016.
[36] M. E. Bauer, "The role of remote sensing in determining the distribution and yield of crops," *Adv. Agronomy*, vol. 27, pp. 271–304, Jan. 1975.
[37] G. Gosal, "Physical geography of the Punjab," *JPS*, vol. 11, no. 1, p. 20, 2004.
[38] G. C. Hulley and S. J. Hook, "Generating consistent land surface temperature and emissivity products between ASTER and MODIS data for earth science research," *IEEE Trans. Geosci. Remote Sens.*, vol. 49, no. 4, pp. 1304–1315, Apr. 2011.
[39] S. A. Ackerman, K. I. Strabala, W. P. Menzel, R. A. Frey, C. C. Moeller, and L. E. Gumley, "Discriminating clear sky from clouds with MODIS," *J. Geophys. Res., Atmos.*, vol. 103, no. D24, pp. 32141–32157, 1998.
[40] G. C. Miliaresis, "Iterative selective spatial variance reduction of MYD11A2 LST data," *Earth Sci. Informat.*, vol. 10, no. 1, pp. 15–27, 2017.
[41] W. G. M. Bastiaanssen, M. J. M. Cheema, W. W. Immerzeel, I. Miltenburg, and H. Pelgrum, "Surface energy balance and actual evapotranspiration of the transboundary Indus Basin estimated from satellite measurements and the ETLook model," *Water Resour. Res.*, vol. 48, no. 11, p. W1151, 2012.
[42] X. Zeng and E. Lu, "Globally unified monsoon onset and retreat indexes," *J. Climate*, vol. 17, pp. 2241–2248, Jun. 2004.
[43] R. Nemani, L. Pierce, S. Running, and S. Goward, "Developing satellite-derived estimates of surface moisture status," *J. Appl. Meteorol.*, vol. 32, pp. 548–557, Mar. 1993.

JAHANGIR KHAN received the B.Sc. degree from the University of Peshawar, Pakistan, in 2000, and the M.S. degree from the Institute of Information and Communication Technology, University of Sindh, Pakistan, in 2004. He is currently pursuing the Ph.D. degree with the College of Information and Electrical Engineering, China Agricultural University, Beijing, China. He is an Assistant Professor with the Faculty of Computer Science and IT, Sarhad University of Science and Information Technology, Peshawar, Pakistan, and on study leave. His research interests include quantitative remote sensing to determine the land surface temperature, drought, and flood as well as to validate the satellite imagery in a geospatial manner regionally.

PENGXIN WANG received the B.S. and M.S. degrees from Northwestern Agricultural University, China, in 1988 and 1991, respectively, and the Ph.D. degree in photogrammetry and remote sensing from Wuhan University, China, in 2001. He was a Post-Doctorate Fellow specializing in the remote-sensing application at the Research Center for Remote Sensing and the Department of Geography, Beijing Normal University, China. He was a Post-Graduate Researcher in the area of remote-sensing application at the Institute of Computational Earth Science, University of California at Santa Barbara, Santa Barbara, CA, USA, from 2001 to 2002. He is currently a Professor with the Department of Geography and Information Engineering, and the Director of the Key Laboratory of Remote Sensing for Agri-Hazards, Ministry of Agriculture, Beijing, at the College of Information and Electrical Engineering, China Agricultural University, China. He invents a near-real-time drought monitoring approach called vegetation temperature condition index model to monitor and determine the drought, and approaches on drought forecasting, winter wheat yield forecasting, LAI and up-scaling regionally and globally. He introduces a geospatial model for the validation of drought using soil moisture and precipitation anomaly. He completed 19 projects from 2002 to 2015 in the area of remote-sensing and currently, two projects are in the tube. He published dozens of refereed articles in reputed journals.

YI XIE received the B.Sc. degree in geographic information systems from Shanxi Agricultural University, Jinzhong, China, in 2012. He is currently pursuing the Ph.D. degree with China Agricultural University, Beijing, China. His main research interests include quantitative remote sensing and its applications in wheat yield estimation.

LEI WANG received the B.S. degree from the School of Resource Environment and Earth Science, Yunnan University, China, in 2012, and the M.S. degree from the College of Information and Electrical Engineering, China Agricultural University, Beijing, China, in 2015, where she is currently pursuing the Ph.D. degree. She is currently a Visiting Student with the Department of Geographical Sciences, University of Maryland at College Park, College Park, MD, USA. Her research interests include quantitative remote sensing.

LI LI received the B.Sc. and M.Sc. degrees in physics and automation from Northeastern University, Shenyang, China, in 1999 and 2002, respectively, and the Ph.D. degree in communication and information system from the Institute of Electronics, Chinese Academy of Science, Beijing, China, in 2005. She is currently an Associate Professor with the College of Information and Electrical Engineering, China Agricultural University, Beijing. She teaches microwave engineering at the undergraduate levels. Her main research interests include the application of microwave remote sensing in agriculture.